Generic scaled versus subject-specific models for the calculation of musculoskeletal loading in cerebral palsy gait
Effect of personalized musculoskeletal geometry outweighs the effect of personalized neural control

Kainz, Hans; Wesseling, Mariska; Jonkers, Ilse

Citation (APA)
Kainz, H., Wesseling, M., & Jonkers, I. (2021). Generic scaled versus subject-specific models for the calculation of musculoskeletal loading in cerebral palsy gait: Effect of personalized musculoskeletal geometry outweighs the effect of personalized neural control. *Clinical Biomechanics*, *87*, Article 105402. https://doi.org/10.1016/j.clinbiomech.2021.105402

Important note
To cite this publication, please use the final published version (if applicable).
Please check the document version above.

Generic scaled versus subject-specific models for the calculation of musculoskeletal loading in cerebral palsy gait: Effect of personalized musculoskeletal geometry outweighs the effect of personalized neural control

Hans Kainz [a,*], Mariska Wesseling [b,c], Ilse Jonkers [b]

[a] *Centre for Sport Science and University Sports, Department of Biomechanics, Kinesiology and Computer Science in Sport, Neuromechanics Research Group, University of Vienna, Austria*
[b] *Human Movement Biomechanics Research Group, KU Leuven, Belgium*
[c] *Faculty of Mechanical, Maritime and Materials Engineering, Department of Biomechanical Engineering, Biomechatronics and Human-Machine Control, TU Delft, Netherlands*

ARTICLE INFO

ABSTRACT

Background: Musculoskeletal modelling is used to assess musculoskeletal loading during gait. Linear scaling methods are used to personalize generic models to each participant's anthropometry. This approach introduces simplifications, especially when used in paediatric and/or pathological populations. This study aimed to compare results from musculoskeletal simulations using various models ranging from linear scaled to highly subject-specific models, i.e., including the participant's musculoskeletal geometry and electromyography data.
Methods: Magnetic resonance images (MRI) and gait data of one typically developing child and three children with cerebral palsy were analysed. Musculoskeletal simulations were performed to calculate joint kinematics, joint kinetics, muscle forces and joint contact forces using four modelling frameworks: 1) Generic-scaled model with static optimization, 2) Generic-scaled model with an electromyography-informed approach, 3) MRI-based model with static optimization, and 4) MRI-based model with an electromyography-informed approach.
Findings: Root-mean-square-differences in joint kinematics and kinetics between generic-scaled and MRI-based models were below 5° and 0.15 Nm/kg, respectively. Root-mean-square-differences over all muscles was below 0.2 body weight for every participant. Root-mean-square-differences in joint contact forces between the different modelling frameworks were up to 2.2 body weight. Comparing the simulation results from the typically developing child with the results from the children with cerebral palsy showed similar root-mean-square-differences for all modelling frameworks.
Interpretation: In our participants, the impact of MRI-based models on joint contact forces was higher than the impact of including electromyography. Clinical reasoning based on overall root-mean-square-differences in musculoskeletal simulation results between healthy and pathological participants are unlikely to be affected by the modelling choice.

1. Introduction

Musculoskeletal simulations have been used to answer research questions on musculoskeletal loading in paediatric and pathological populations (Kainz et al., 2020; Steele et al., 2012b; Wesseling et al., 2016). Typically a generic musculoskeletal model developed from cadaveric data of an adult is scaled to the anthropometry of the child (Delp et al., 2007). This procedure neglects subject-specific musculoskeletal geometry, e.g., subject and age-specific femoral neck-shaft angle (Bobroff et al., 1999). To overcome these limitations, musculoskeletal models can be generated from medical images of the participants (Kainz et al., 2016; Scheys et al., 2008; Valente et al., 2017). In children with cerebral palsy (CP), only a small number of studies have compared generic scaled with medical imaging-based models. These studies

Table 1

Summary of participant's anthropometrical parameters and spasticity scores. Spasticity was graded with the Modified Ashworth Scale. R = right; L = left; CP = cerebral palsy; ♂ = male; ♀ = female. Anteversion and neck-shaft angles were measured from the segmented femur of the MRI images using a customized Matlab code.

	TD		CP1		CP2		CP3	
Gender	♂		♀		♂		♂	
Age (years)	8		14		9		15	
Height (m)	1.24		1.44		1.31		1.71	
Weight (kg)	20.4		43.4		32.2		49.1	
Diagnosis	Healthy		Diplegic CP		Diplegic CP		Diplegic CP	
Femoral geometry	R	L	R	L	R	L	R	L
Anteversion angle (°)	18.2	25.5	33.9	21.0	39.7	30.9	23.1	22.0
Neck-shaft angle (°)	127.0	133.6	139.9	136.9	127.0	134.4	132.3	126.2
Spasticity	R	L	R	L	R	L	R	L
Hip flexors	–	–	1	1.5	1	0	1	1
Hip adductors	–	–	1.5	1.5	0	0	1.5	1
Hamstrings	–	–	1.5	1.5	1.5	1.5	1.5	2
Soleus	–	–	1	1.5	1.5	1.5	1.5	1.5
Gastrocnemius	–	–	2	2	1.5	1.5	2	2
Tibialis posterior	–	–	0	0	0	0	1	0
Overall score	0	0	7	8	5.5	4.5	8.5	7.5

reported differences in muscle moment arms (Correa et al., 2011; Scheys et al., 2008), hip joint contact force orientation (Bosmans et al., 2014) and joint kinematics (Scheys et al., 2011) between generic scaled and medical imaging based models.

Although the medical imaging-based models from the above-mentioned studies account for the abnormal musculoskeletal geometry, they neglected the impaired motor control that is present in children with cerebral palsy (CP). The impaired motor control will not influence the calculated joint kinematics and kinetics but may impact muscle and joint contact force (JCF) estimations. Muscle forces are typically estimated using static optimization, which assumes identical neuromuscular control strategies between individuals and tasks in the muscle force distribution algorithm. This approach, however, might not be appropriate for participants with neurological disorders. Including electromyography (EMG) data collected from the participant in the estimation of muscle forces can overcome this limitation (Lloyd and Besier, 2003; Wesseling et al., 2020). Muscle activation profile obtained with this so-called EMG-informed approaches have been shown to better resemble the measured EMG signals (Hoang et al., 2018). Despite these advantages, few studies have applied EMG-informed approaches when studying children with CP (Falisse et al., 2020; Kainz et al., 2019; Veerkamp et al., 2019). Furthermore, to the best of the authors' knowledge, no studies combined medical-imaging based models with an EMG-informed approach to estimate the effect of geometry versus motor control on estimations of muscle and JCF.

To assess the relevance of the differences between workflows, we need to consider their impact on clinical reasoning. In a clinical context, patient data is usually compared to reference data of a healthy population. Measurements based on root-mean-square-differences (RMSD) between the patient and healthy reference waveforms have therefore been proposed to summarize joint angle (Baker et al., 2009), joint moment (Cimolin et al., 2019), and muscle force (Kainz et al., 2019) deviations to support clinical decision-making to restore gait and musculoskeletal loading. The impact of the modelling framework on clinical reasoning, in terms of the RMSD between the patient and reference waveforms has not been studied comprehensively.

In a clinical context, collecting the necessary data and generating fully subject-specific models is rarely possible due to the lack of resources (i.e., time, money, knowledge, limited attention span and tolerance of children). Knowing the impact of excluding subject-specific information on simulation results is, therefore, essential for choosing the appropriate modelling framework still allowing to answer clinical

research questions. Hence, the aim of this study was to compare simulation results from highly subject-specific models, which include the participant's musculoskeletal geometry as well as EMG data, with less sophisticated models of generic geometry and motor control. Considering that the inclusion of EMG data will not affect joint kinematics and kinetics whereas the inclusion of MRI data will have an impact on all musculoskeletal simulation results (from joint kinematics to contact forces), we hypothesized that the inclusion of personalized geometry (MRI data) will have a bigger impact on simulation results than the inclusion of personalized neural control (EMG data). Furthermore, we assessed the impact of the modelling choice on clinical-reasoning in terms of RMSD between children with CP and a typically developing participant.

2. Methods

2.1. Participants

Gait data and magnetic resonance images (MRI) of one typically developing (TD) child and three children with CP (Table 1) were analysed for this study. The CP participants covered a wide range of clinical-relevant deviation in femoral geometry and spasticity scores. In CP participants, lower limb muscle spasticity was assessed using the Modified Ashworth Scale (Bohannon and Smith, 1987). Ethical approval was obtained from the local ethics committee (UZ Leuven, Belgium, S57746).

2.2. Motion capture

Vicon Plug-in-Gait lower limb marker set (Kadaba et al., 1990) with additional three marker clusters on the thighs and shanks and an additional foot marker on the 5th metatarsal head were placed on each participant. Marker trajectories and ground reaction forces of one static and at least three walking trials at a self-selected walking speed were collected with an 8–15 camera motion capture system (Vicon Motion Systems, Oxford, UK) and two force plates (AMTI, Watertown, MA, USA). Simultaneously, EMG data was collected using a 16-channel EMG-system (Zerowire, Cometa, Italy). In CP participants, surface EMG signals of following lower limb muscles were collected bilaterally: rectus femoris, vastus lateralis, biceps femoris, semitendinosous, tibialis anterior, medial gastrocnemicus, soleus and gluteus medius. The TD participant only had EMG on following muscles of the right leg: rectus
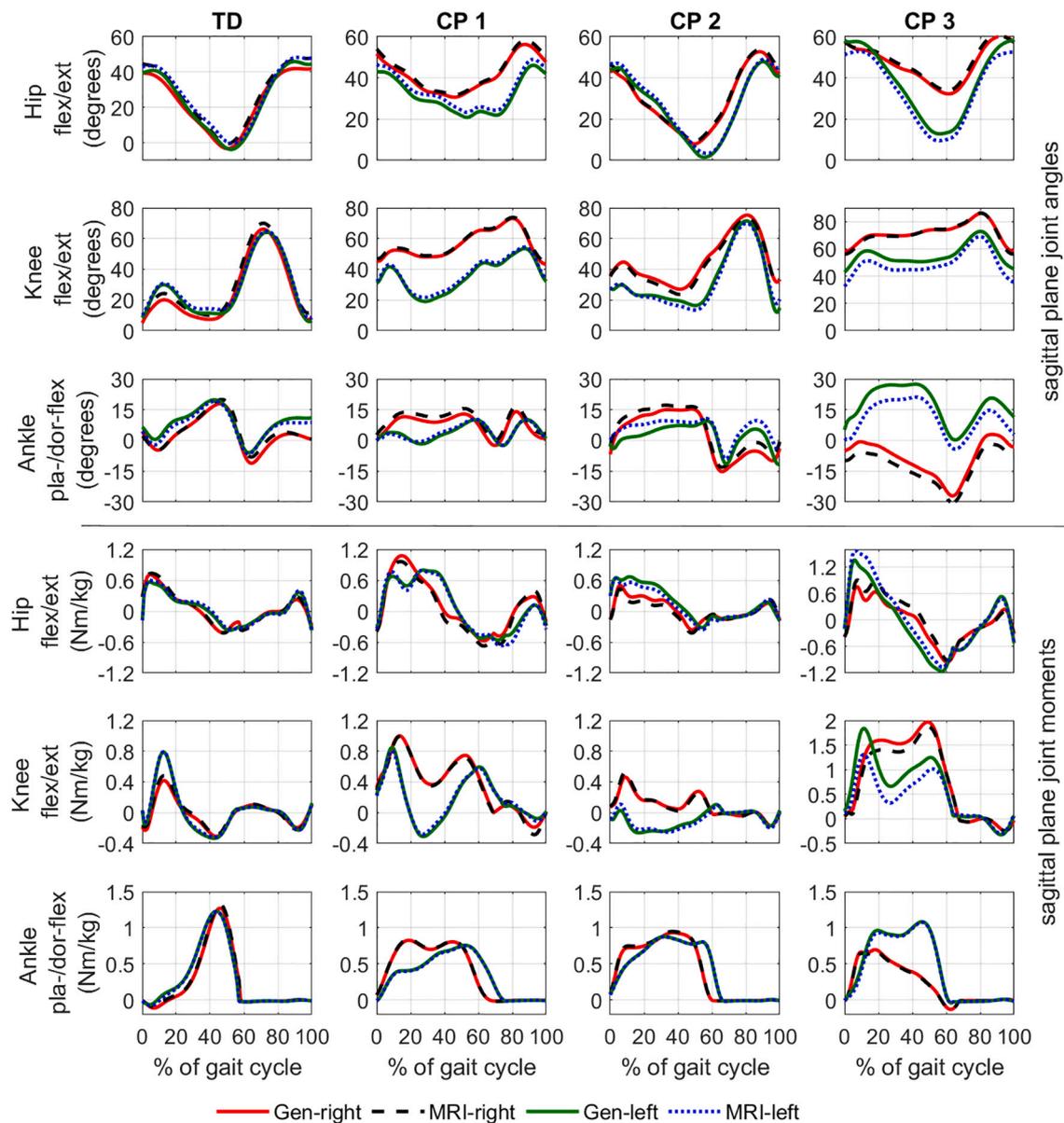
Fig. 1. Sagittal plane joint kinematics (first three rows) and joint kinetics (bottom three rows) from all participants obtained with the generic-scaled (solid waveforms) and MRI-based models (dashed and dotted waveforms).

femoris, vastus lateralis and medialis, biceps femoris, semitendinosus, medial and lateral gastrocnemicus, sartorius and gracilis. Vicon Nexus 2.1 (Vicon Motion Systems, Oxford, UK) was used to label and filter marker trajectories and filter force plate data, with filters being a Butterworth 4th order zero-lag dual-pass, low pass filter with a cut-off frequency of 6 Hz. EMG was band-pass filtered between 20 and 400 Hz, rectified, low-pass filtered at 10 Hz and normalized to the maximum value within the gait trial.

2.3. MRI acquisition

MRI were collected using 1.5 T magnetic resonance scanner (either the MAGNETOM Avanto scanner, Siemens, Germany or Philips MRI scanner, Philips Electronics, UK). A full lower-body scan including the pelvis and bones of the lower limbs were obtained from each participant in a supine position (Scheys et al., 2006). Prior to the scan, MRI compatible and opaque markers were placed on anatomical landmarks according to the motion capture marker protocol.

2.4. Musculoskeletal models and simulations

For each participant, a MRI-based and a generic-scaled OpenSim model (Delp et al., 1990) were created based on a previously developed workflow (Scheys et al., 2006) and included following steps: (1) The pelvis, femurs, tibias and fibulas were segmented using Mimics (Materialise, Leuven, Belgium). (2) The segmented bones were imported into an in-house developed software to build musculoskeletal SIMM models based on medical images. Afterwards, anatomical reference frames, joints and the muscle lines of action were defined based on the MRI images. (3) The final SIMM model was converted to an OpenSim model. (4) OpenSim's scaling/marker placer tool was used to move the cluster markers, which were not attached during the MRI scans, to their correct positions using segment markers, visible in both motion capture and MRI trials, as a reference. For the generic-scaled model (Gen), a SIMM model with the same joint degrees of freedom and anatomical reference frame definitions as the MRI-model was converted to an OpenSim model and scaled to the anthropometry of each child based on the experimental marker positions and estimated joint centres (Kainz et al., 2017).
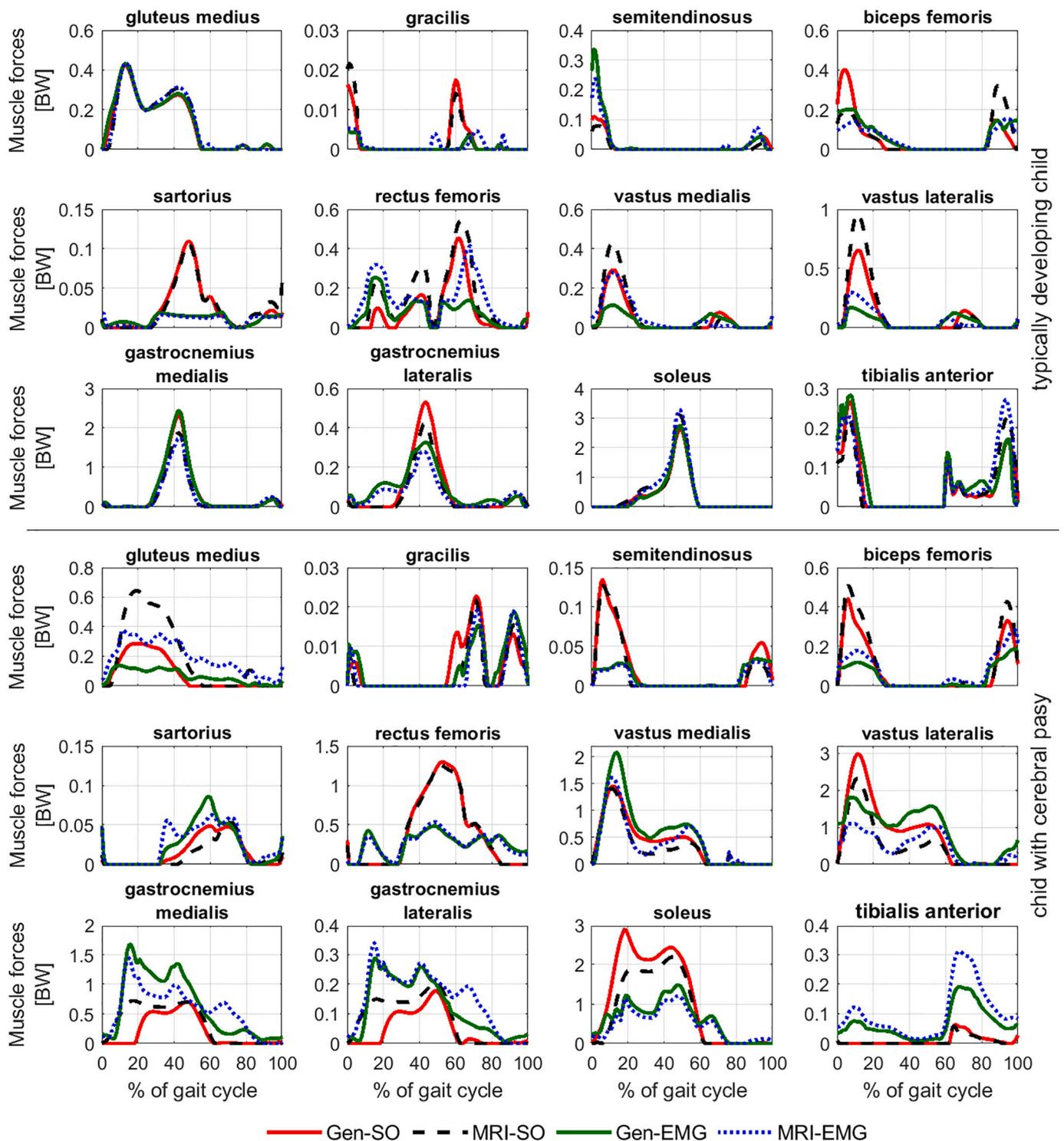
Fig. 2. A selection of muscle forces from the typically developing participant (first three rows) and one participant with CP (bottom three rows) calculated with all four different modelling approaches.

OpenSim 3.3 (Delp et al., 2007) was used to calculate joint angles, joint moments, muscle and JCF. Joint angles and moments were calculated using a Kalman smoother (De Groote et al., 2008) and inverse dynamics, respectively. Muscle forces were estimated using two approaches: (1) Static optimization (SO), which minimizes the sum of squared muscle activations and is one of the most common ways to calculate muscle forces in OpenSim (Delp et al., 2007) and (2) EMG-constrained SO (Wesseling et al., 2020), which used the processed EMG signal as input to constrain the estimated muscle activation pattern. Due to the lack of

trials with maximum muscle activations, an activation scale factor for each EMG signal was minimized within the cost function. Constrained muscle activations were permitted to deviate from the scaled EMG signal by maximally 10%. Muscles for which EMG signals were not available were free to vary within the optimization, which minimized the sum of squared muscle activations. Afterwards, joint contact forces were estimated using OpenSim's joint reaction analysis (Steele et al., 2012a). Combining the two different models and two different optimization approaches led to following four modelling frameworks:
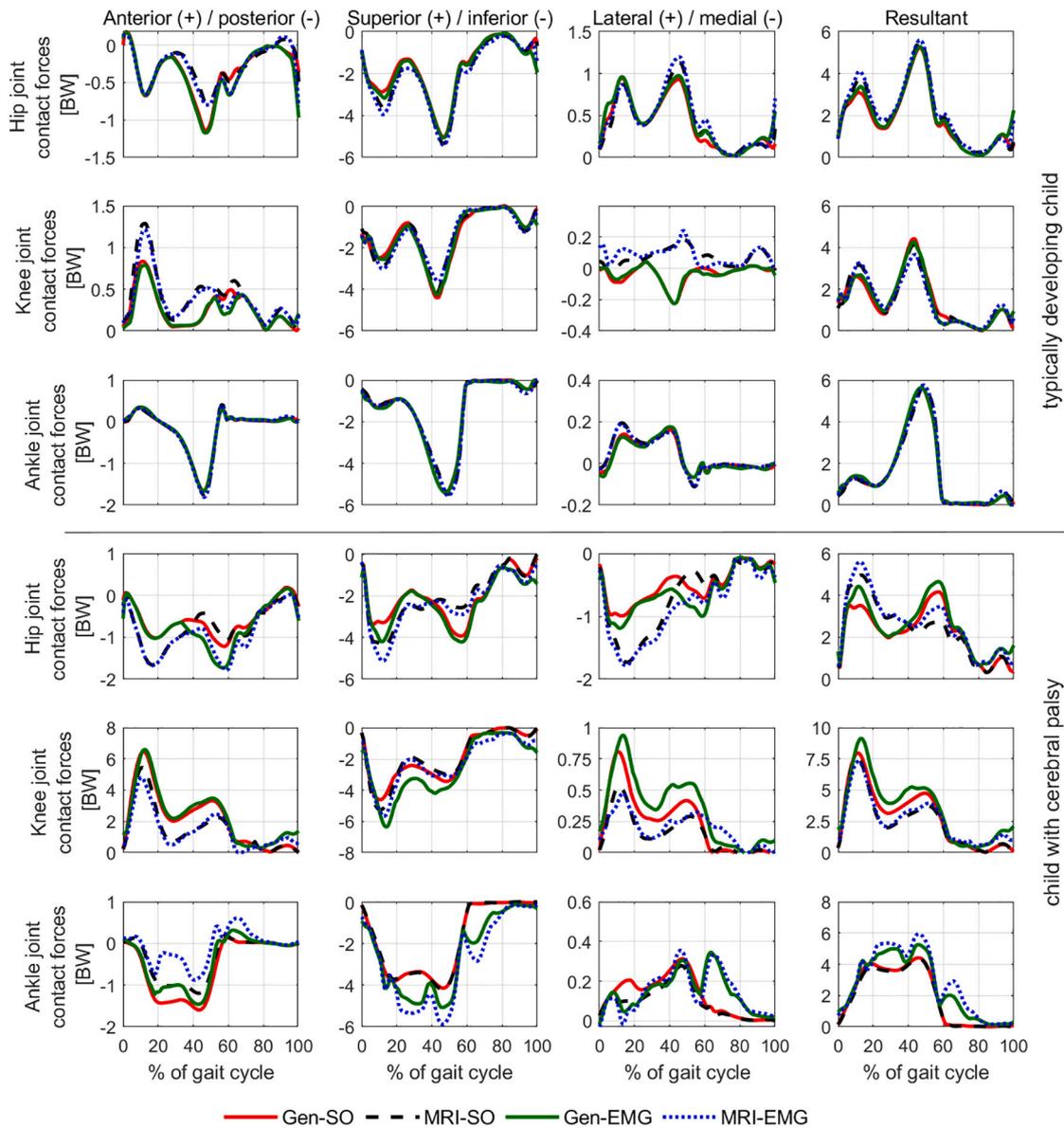
Fig. 3. Hip, knee and ankle joint contact forces from the typically developing participant (first three rows) and one participant with CP (bottom three rows) calculated with all four different modelling approaches.

- Gen-SO: Generic-scaled model in combination with SO, lacking personalized musculoskeletal geometry and control;
- MRI-SO: MRI-based model in combination with SO, reflecting personalized musculoskeletal geometry but not control;
- Gen-EMG: Generic-scaled model in combination with the EMG constrained approach, lacking personalized musculoskeletal geometry but reflecting personalized control
- MRI-EMG: MRI-based model in combination with the EMG constrained approach reflecting personalized musculoskeletal geometry as well as control;

Joint kinematics, joint kinetics, muscle and JCF were compared between all modelling frameworks.

2.5. Data analysis

The right and left leg of each child were analysed separately. For each participant, joint angle, joint moment, muscle force and JCF waveforms were calculated over the gait-cycle using all modelling frameworks. RMSD were used to compare waveforms between the different modelling frameworks. To address our hypothesis (MRI has a bigger impact on simulation results than EMG), we compared the differences caused by the inclusion of MRI (Gen-EMG versus MRI-EMG) and EMG data (MRI-SO versus MRI-EMG) using either a paired t-tests or Wilcoxon test, depending on the distribution of our data. Normal distribution was assessed using the Kolmogorov-Smirnov test in SPSS Statistics v23 (IBM Corporation, New York, USA). To investigate the impact of modelling and simulation choice on clinical reasoning, we calculated RMSD between the simulation results from the TD child and each CP child using all modelling frameworks.

3. Results

Joint kinematics and kinetics of the TD child showed typical waveforms for unimpaired gait and were in agreement with previous research (Schwartz et al., 2008). All CP participants walked with an increased hip and knee flexion angle (Fig. 1). RMSD in joint kinematics and kinetics between the generic-scaled and MRI models were below 5° and 0.12 Nm/kg, respectively (Fig. 4).

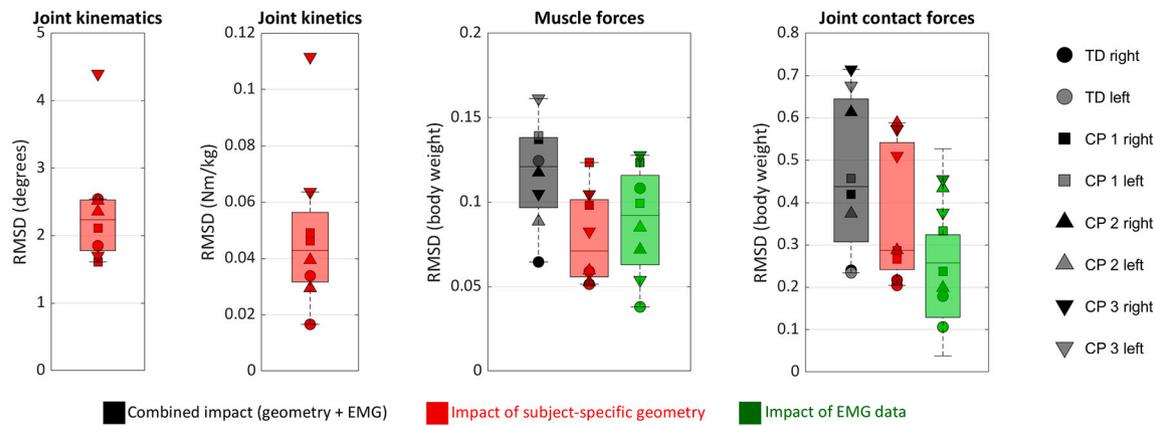Shape and magnitude of muscle and JCF of the TD participant

Fig. 4. Average root-mean-square-differences (RMSD) in joint kinematics, joint kinetics, muscles forces and joint contact forces between the MRI-EMG model and the Gen-SO (black symbols), Gen-EMG (red symbols) and MRI-SO (green symbols) models. The red symbols show the RMSD due to the inclusion of subject-specific geometry, whereas the greem symbols show the RMSD due to the inclusion of EMG data in the estimation of muscle forces. The black symbols show the combined impact due to the inclusion of subject-specific geometry and EMG data. (For interpretation of the references to colour in this figure legend, the reader is referred to the web version of this article.)

(Figs. 2 and 3) were similar to previous studies which used MRI-based models in paediatric populations (Bosmans et al., 2014; Modenese et al., 2018). The impact of the modelling framework on estimated muscle forces varied between muscles and participants (Fig. 2). The RMSD over all muscles was below 0.2 body weight (BW) for every participant (Fig. 4). Nevertheless, differences above 200% in maximal individual muscles forces were observed for some muscles (e.g. gluteus medius and semitendinosus in CP3, Fig. 2). Average RMSD in JCF between the different modelling frameworks were below 0.8 BW in all participants (Fig. 4). Hip and knee JCF were sensitive to the inclusion of subject-specific geometry, whereas ankle JCF were more sensitive to the inclusion of EMG data in most CP participants (supplementary Fig. S3).

The impact of including MRI data (Gen-EMG versus MRI-EMG) on JCF (0.31 ± 0.14 BW) was significantly higher (P = 0.036) than the impact due to EMG data (MRI-SO versus MRI-EMG; 0.24 ± 0.11 BW). The comparison of the impact of including MRI or EMG data on estimated muscle forces showed no significant difference. Comparing the musculoskeletal simulation results from the TD child with the results from the CP children showed similar RMSD for all modelling frameworks (Fig. 5).

4. Discussion

The purpose of this investigation was to compare simulation results from highly subject-specific models with less detailed models. We generally found that the modelling choice had a minor impact on joint kinematics and kinetics. Muscle forces and JCF were more sensitive to the modelling choice. Inclusion of personalized geometry had a significant higher impact on JCF than the inclusion of personalized neural control information, which confirmed our hypothesis. Interestingly, the ability to discriminate between TD and CP simulation results, as reflected in the RMSD between TD and CP participants, was similar between the modelling frameworks.

Joint kinematics were very similar between our MRI and generic-scaled models (overall RMSD below 5°). Considering the small differences in joint kinematics between models, the minor differences in joint kinetics were not surprising. Previous research showed that joint kinematics is mainly influenced by different anatomical segment frame definitions and joint degree-of-freedoms (Kainz et al., 2016). Our MRI and generic-scaled models were based on similar segment and joint definitions and therefore explains the minor impact on joint kinematics.

The impact of subject-specific geometry on muscle and JCF was not as straight forward as expected. For example, the femoral geometry, i.e. anteversion angle and neck-shaft angle, of the left leg from CP3 was only

slightly different (less than 5°) from the geometry of the generic-scaled model but the impact of the inclusion of subject-specific geometry on hip JCF was higher than in all other participants (supplementary Fig. S3). In CP3, joint kinematics of the left leg showed already big differences between the generic-scaled and MRI models, indicating that the differences in hip JCF are due to a summation of differences caused at each step of the simulation workflow. Femoral segment length of CP3 differed by 18 mm between the generic-scaled and MRI-based model, which was larger compared to our other participants (11 mm ± 5 mm). Different segment lengths have been shown to impact simulation results (Koller et al., 2021) and might explain the high impact on hip JCF in CP3. Furthermore, the impact of the chosen modelling framework on simulation results may depend on the subject-specific walking pattern of each child. Geometrical differences between models will affect the muscle attachment and via points and therefore the moment arms of specific muscles (Wesseling et al., 2019), but this will only affect muscle and JCF estimates if these muscles are major contributors (i.e., highly active) to the person's gait.

Subject-specific motor control affected the simulation results and showed, as expected, a higher impact of an EMG informed approach on JCF in the presence of more spastic muscles (supplementary Fig. S4). The impact of including EMG data was higher on the ankle JCF than on the hip and knee JCF. Soleus and calf muscles were the most spastic muscle in all our participants with CP, which might explain the high impact on ankle JCF.

In a clinical context, it is common to compare the patient's waveforms to reference waveforms from a TD population and summarize the results using RMSD. When comparing the musculoskeletal modelling results from our CP participants with our TD participant, we found similar RMSD for all modelling frameworks. For example, the right leg of CP3 showed the largest deviation from the TD child independent of the chosen modelling framework. This is in agreement with Correa et al. (2011), who found consistent muscles functions between generic-scaled and MRI-based models, and Kainz et al. (2019), who found similar deviations in muscle forces when using an EMG-informed approach compared to static optimization.

The impact of subject-specific geometry on overall JCF was higher than the impact of subject-specific neural control. The impact of MRI or EMG data on muscle forces, however, was not different. Contrary to including MRI, including EMG data does not change joint kinematics. Considering that JCF calculations take the angular and linear accelerations of segments into account, it is not surprising that the impact of MRI on JCF was higher than the impact of EMG data.

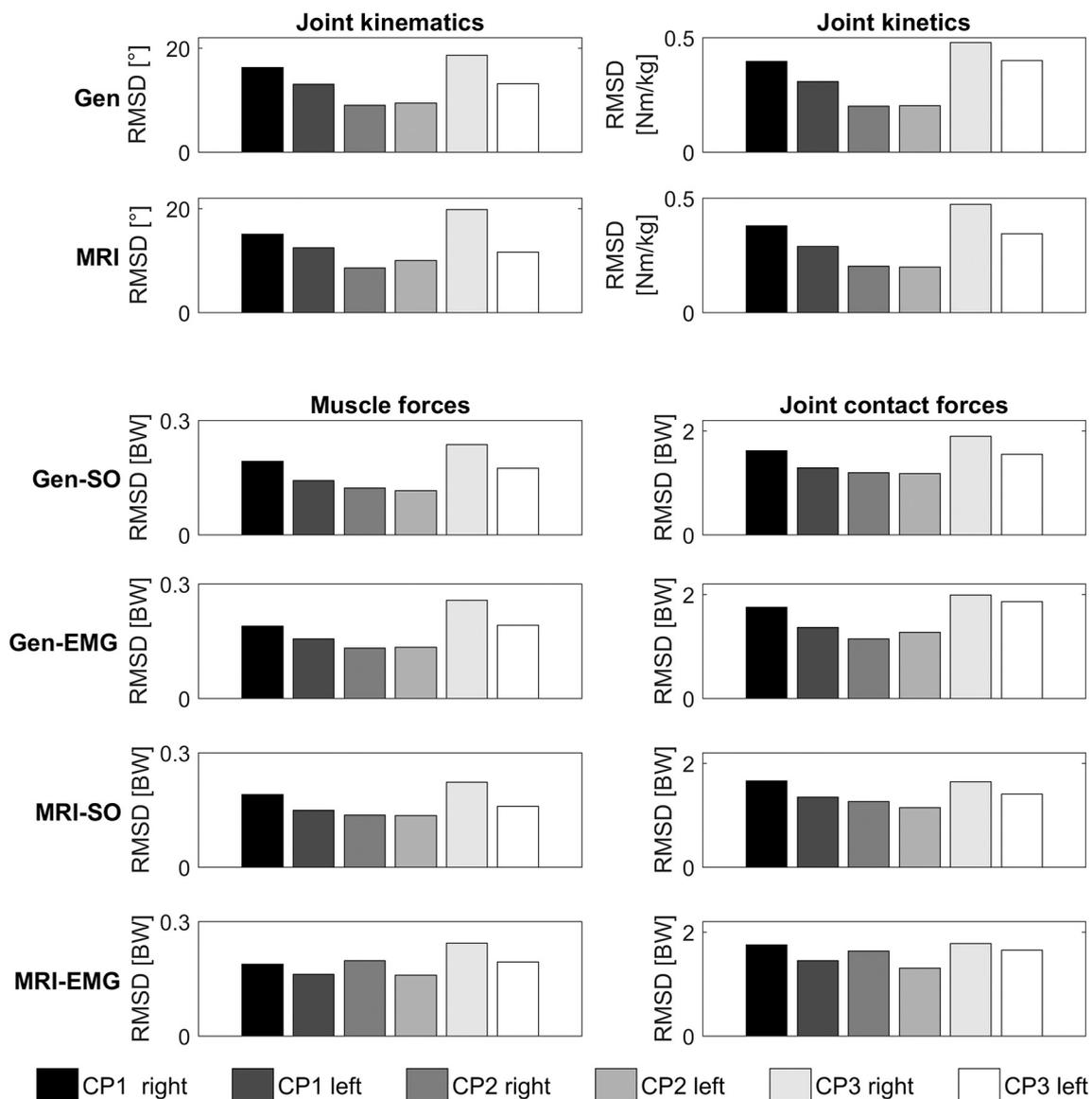Highly subject-specific models have the advantage to account for the

Fig. 5. Root-mean-square-difference (RMSD) between the TD participant and the CP participants waveforms calculated using the generic scaled (Gen) and MRI-based (MRI) models as well as static optimization (SO) and the EMG-constrained (EMG) approach. RMSD between the patient and TD waveforms have been proposed to summarize deviation from TD children and support the clinical decision making.

individual's musculoskeletal geometry and motor control. The creation of highly subject-specific models is, however, not only very time-consuming but also adds uncertainties to the simulations due to the additional parameters needed for the model and running the simulations. The sensitivity of the modelling approaches may inherently be different between EMG-informed and MRI-based models. EMG-informed models are mainly influenced by the EMG signals and chosen optimization method and parameters. The EMG signal depends on a proper placement of the electrodes and the walking pattern of the participant. MRI-based models, on the other hand, mainly depend on the selection of anatomical landmarks from the MRI images and, therefore, are independent of the dynamic movement trials of the participant. Previous studies investigated the sensitivity of parameter identifications for subject-specific musculoskeletal simulations and sowed that most parameters are robust and did not markedly change the simulation results (Hannah et al., 2017; Martelli et al., 2015; Valente et al., 2014). The current development of automated workflows to create highly subject-specific models (Modenese and Kohout, 2020; Modenese and Renault, 2021) will likely improve the repeatability of subject-specific

simulations in the future.

This study includes some limitations. First, due to the time-consuming process of creating subject-specific models, this study only included a small sample size and, therefore, the statistical findings should be interpreted with caution. Second, our findings are based on the collected walking trials of our participants and used musculoskeletal simulation methods. Different movements (e.g. ascending stairs) or different approaches to include EMG data in the musculoskeletal simulations (Pizzolato et al., 2015) might lead to different results. Third, different methods to process the EMG data might influence the results from the EMG informed approaches (Gen-EMG and MRI-EMG). Forth, our statistical analyses were only performed based on RMSD between modelling frameworks but did not include discrete parameters, e.g. peak force of the gastrocnemius muscle. Note that although RMSD were relatively low, some discrete parameters showed large differences between modelling frameworks (Figs. 2 and 3). Furthermore, future studies based on a larger sample size should be conducted to verify our conclusions.

5. Conclusion

Our findings highlight that the impact of modelling choice on simulation results depends on a combination of subject-specific musculoskeletal geometry and motor control rather than the difference in geometry or motor control alone (Fig. 4). The high variability of our results between participants was likely caused by the different walking patterns, which require different muscle forces. The modelling framework will affect moment arms (generic versus MRI) and muscle activations (SO versus EMG-informed optimization), but this will only affect simulation results if these muscles are major contributors to the person's gait. In our participants, the impact of subject-specific geometry on simulation results was higher than the impact of including subject-specific neural control. Clinical reasoning based on overall RMSD in musculoskeletal simulation results between CP and TD participants are unlikely to be affected by the modelling choice. Our results may help peers to estimate and understand differences in simulation results due to certain modelling choices. Models and simulation results are freely available from https://simtk.org/projects/genvssubspec.

Declaration of Competing Interest

The authors declare no conflicts of interest.

Appendix A. Supplementary data

Supplementary data to this article can be found online at https://doi.org/10.1016/j.clinbiomech.2021.105402.

References

Baker, R., McGinley, J.L., Schwartz, M.H., Beynon, S., Rozumalski, A., Graham, H.K., Tirosh, O., 2009. The gait profile score and movement analysis profile. Gait Posture 30, 265–269. https://doi.org/10.1016/J.GAITPOST.2009.05.020.

Bobroff, E.D., Chambers, H.G., Sartoris, D.J., Wyatt, M.P., Sutherland, D.H., 1999. Femoral anteversion and neck-shaft angle in children with cerebral palsy. Clin. Orthop. Relat. Res. 194–204.

Bohannon, R.W., Smith, M.B., 1987. Interrater reliability of a modified Ashworth scale of muscle spasticity. Phys. Ther. 67, 206–207.

Bosmans, L., Wesseling, M., Desloovere, K., Molenaers, G., Scheys, L., Jonkers, I., 2014. Hip contact force in presence of aberrant bone geometry during normal and pathological gait. J. Orthop. Res. 32, 1406–1415. https://doi.org/10.1002/jor.22698.

Cimolin, V., Condoluci, C., Costici, P.F., Galli, M., 2019. A proposal for a kinetic summary measure: the gait kinetic index. Comput. Methods Biomech. Biomed. Engin. 22, 94–99. https://doi.org/10.1080/10255842.2018.1536750.

Correa, T.A., Baker, R., Kerr Graham, H., Pandy, M.G., 2011. Accuracy of generic musculoskeletal models in predicting the functional roles of muscles in human gait. J. Biomech. 44, 2096–2105. https://doi.org/10.1016/j.jbiomech.2011.05.023.

De Groote, F., De Laet, T., Jonkers, I., De Schutter, J., 2008. Kalman smoothing improves the estimation of joint kinematics and kinetics in marker-based human gait analysis. J. Biomech. 41, 3390–3398. https://doi.org/10.1016/j.jbiomech.2008.09.035.

Delp, S.L., Loan, J.P., Hoy, M.G., Zajac, F.E., Topp, E.L., Rosen, J.M., 1990. An interactive graphics-based model of the lower extremity to study orthopaedic surgical procedures. IEEE Trans. Biomed. Eng. 37, 757–767. https://doi.org/10.1109/10.102791.

Delp, S.L., Anderson, F.C., Arnold, A.S., Loan, P., Habib, A., John, C.T., Guendelman, E., Thelen, D.G., 2007. OpenSim: open-source software to create and analyze dynamic simulations of movement. IEEE Trans. Biomed. Eng. 54, 1940–1950. https://doi.org/10.1109/TBME.2007.901024.

Falisse, A., Pitto, L., Kainz, H., Hoang, H., Wesseling, M., Van Rossom, S., Papageorgiou, E., Bar-On, L., Hallemans, A., Desloovere, K., Molenaers, G., Van Campenhout, A., De Groote, F., Jonkers, I., 2020. Physics-based simulations to predict the differential effects of motor control and musculoskeletal deficits on gait dysfunction in cerebral palsy: a retrospective case study. Front. Hum. Neurosci. 14, 40. https://doi.org/10.3389/fnhum.2020.00040.

Hannah, I., Montefiori, E., Modenese, L., Prinold, J., Viceconti, M., Mazzà, C., 2017. Sensitivity of a juvenile subject-specific musculoskeletal model of the ankle joint to

the variability of operator-dependent input. Proc. Inst. Mech. Eng. Part H J. Eng. Med. 231, 415–422. https://doi.org/10.1177/0954411917701167.

Hoang, H.X., Pizzolato, C., Diamond, L.E., Lloyd, D.G., 2018. Subject-specific calibration of neuromuscular parameters enables neuromusculoskeletal models to estimate physiologically plausible hip joint contact forces in healthy adults. J. Biomech. 80, 111–120. https://doi.org/10.1016/J.JBIOMECH.2018.08.023.

Kadaba, M.P., Ramakrishnan, H.K., Wootten, M.E., 1990. Measurement of lower extremity kinematics during level walking. J. Orthop. Res. 8, 383–392. https://doi.org/10.1002/jor.1100080310.

Kainz, H., Modenese, L., Lloyd, D.G., Maine, S., Walsh, H.P.J., Carty, C.P., 2016. Joint kinematic calculation based on clinical direct kinematic versus inverse kinematic gait models. J. Biomech. 49, 1658–1669. https://doi.org/10.1016/j.jbiomech.2016.03.052.

Kainz, H., Hoang, H., Stockton, C., Boyd, R.R., Lloyd, D.G., Carty, C.P., 2017. Accuracy and reliability of marker based approaches to scale the pelvis, thigh and shank segments in musculoskeletal models. J. Appl. Biomech. 1–21 https://doi.org/10.1123/jab.2016-0282.

Kainz, H., Hoang, H., Pitto, L., Wesseling, M., Van Rossom, S., Van Campenhout, A., Molenaers, G., De Groote, F., Desloovere, K., Jonkers, I., 2019. Selective dorsal rhizotomy improves muscle forces during walking in children with spastic cerebral palsy. Clin. Biomech. (Bristol, Avon) 65, 26–33. https://doi.org/10.1016/j.clinbiomech.2019.03.014.

Kainz, H., Killen, B.A., Wesseling, M., Perez-Boerema, F., Pitto, L., Garcia Aznar, J.M., Shefelbine, S., Jonkers, I., 2020. A multi-scale modelling framework combining musculoskeletal rigid-body simulations with adaptive finite element analyses, to evaluate the impact of femoral geometry on hip joint contact forces and femoral bone growth. PLoS ONE 15, e0235966. https://doi.org/10.1371/journal.pone.0235966.

Koller, W., Baca, A., Kainz, H., 2021. Impact of scaling errors of the thigh and shank segments on musculoskeletal simulation results. Gait Posture 87, 65–74. https://doi.org/10.1016/j.gaitpost.2021.02.016.

Lloyd, D.G., Besier, T.F., 2003. An EMG-driven musculoskeletal model to estimate muscle forces and knee joint moments in vivo. J. Biomech. 36, 765–776. https://doi.org/10.1016/S0021-9290(03)00010-1.

Martelli, S., Valente, G., Viceconti, M., Taddei, F., 2015. Sensitivity of a subject-specific musculoskeletal model to the uncertainties on the joint axes location. Comput. Methods Biomech. Biomed. Engin. 18, 1555–1563. https://doi.org/10.1080/10255842.2014.930134.

Modenese, L., Kohout, J., 2020. Automated generation of three-dimensional complex muscle geometries for use in personalised musculoskeletal models. Ann. Biomed. Eng. 48, 1793–1804. https://doi.org/10.1007/s10439-020-02490-4.

Modenese, L., Renault, J.B., 2021. Automatic generation of personalised skeletal models of the lower limb from three-dimensional bone geometries. J. Biomech. 116, 110186. https://doi.org/10.1016/j.jbiomech.2020.110186.

Modenese, L., Montefiori, E., Wang, A., Wesarg, S., Viceconti, M., Mazzà, C., 2018. Investigation of the dependence of joint contact forces on musculotendon parameters using a codified workflow for image-based modelling. J. Biomech. 73, 108–118. https://doi.org/10.1016/j.jbiomech.2018.03.039.

Pizzolato, C., Lloyd, D.G., Sartori, M., Ceseracciu, E., Besier, T.F., Fregly, B.J., Reggiani, M., 2015. CEINMS: a toolbox to investigate the influence of different neural control solutions on the prediction of muscle excitation and joint moments during dynamic motor tasks. J. Biomech. 48, 3929–3936. https://doi.org/10.1016/j.jbiomech.2015.09.021.

Scheys, L., Jonkers, I., Loeckx, D., Maes, F., Spaepen, A., Suetens, P., 2006. Image Based Musculoskeletal Modeling Allows Personalized Biomechanical Analysis of Gait. Springer, Berlin, Heidelberg, pp. 58–66. https://doi.org/10.1007/11790273_7.

Scheys, L., Van Campenhout, A., Spaepen, A., Suetens, P., Jonkers, I., 2008. Personalized MR-based musculoskeletal models compared to rescaled generic models in the presence of increased femoral anteversion: effect on hip moment arm lengths. Gait Posture 28, 358–365. https://doi.org/10.1016/J.GAITPOST.2008.05.002.

Scheys, L., Desloovere, K., Spaepen, A., Suetens, P., Jonkers, I., 2011. Calculating gait kinematics using MR-based kinematic models. Gait Posture 33, 158–164. https://doi.org/10.1016/j.gaitpost.2010.11.003.

Schwartz, M.H., Rozumalski, A., Trost, J.P., 2008. The effect of walking speed on the gait of typically developing children. J. Biomech. 41, 1639–1650. https://doi.org/10.1016/j.jbiomech.2008.03.015.

Steele, K.M., DeMers, M.S., Schwartz, M.H., Delp, S.L., 2012a. Compressive tibiofemoral force during crouch gait. Gait Posture 35, 556–560. https://doi.org/10.1016/J.GAITPOST.2011.11.023.

Steele, K.M., van der Krogt, M.M., Schwartz, M.H., Delp, S.L., 2012b. How much muscle strength is required to walk in a crouch gait? J. Biomech. 45, 2564–2569. https://doi.org/10.1016/j.jbiomech.2012.07.028.

Valente, G., Pitto, L., Testi, D., Seth, A., Delp, S.L., Stagni, R., Viceconti, M., Taddei, F., 2014. Are subject-specific musculoskeletal models robust to the uncertainties in parameter identification? PLoS ONE 9, e112625. https://doi.org/10.1371/journal.pone.0112625.

Valente, G., Crimi, G., Vanella, N., Schileo, E., Taddei, F., 2017. nmsBuilder: freeware to create subject-specific musculoskeletal models for OpenSim. Comput. Methods Programs Biomed. 152, 85–92. https://doi.org/10.1016/j.cmpb.2017.09.012.

Veerkamp, K., Schallig, W., Harlaar, J., Pizzolato, C., Carty, C.P., Lloyd, D.G., van der Krogt, M.M., 2019. The effects of electromyography-assisted modelling in estimating musculotendon forces during gait in children with cerebral palsy. J. Biomech. https://doi.org/10.1016/J.JBIOMECH.2019.05.026.

Wesseling, M., Meyer, C., Corten, K., Simon, J.-P., Desloovere, K., Jonkers, I., 2016. Does surgical approach or prosthesis type affect hip joint loading one year after surgery? Gait Posture 44, 74–82. https://doi.org/10.1016/j.gaitpost.2015.11.009.

Wesseling, M., Bosmans, L., Van Dijck, C., Vander Sloten, J., Wirix-Speetjens, R., Jonkers, I., 2019. Non-rigid deformation to include subject-specific detail in musculoskeletal models of CP children with proximal femoral deformity and its

effect on muscle and contact forces during gait. Comput. Methods Biomech. Biomed. Engin. 22, 376–385. https://doi.org/10.1080/10255842.2018.1558216.

Wesseling, M., Kainz, H., Hoekstra, T., Van Rossom, S., Desloovere, K., De Groote, F., Jonkers, I., 2020. Botulinum toxin injections minimally affect modelled muscle forces during gait in children with cerebral palsy. Gait Posture 82, 54–60. https://doi.org/10.1016/j.gaitpost.2020.08.122.